NHERP AWARD 04HQGR0121
Final Technical Report

HONEY LAKE AND FT. SAGE MOUNTAINS FAULT ZONES: POTENTIAL CONSTRAINT ON ATTENUATION RELATIONSHIPS FOR STRONG GROUND MOTIONS IN EXTENSIONAL REGIMES.

Steven G. Wesnousky
Center for Neotectonic Studies
University of Nevada, Reno
MS 169
Reno, NV 89557
775-784-6067 (tel), 775-784-1382 (fax)
stevew@seismo.unr.edu
http:// neotectonics.seismo.unr.edu

Program Element: NIW
Key words: Strong ground motion, attenuation relations, neotectonics, trench investigations, paleseismology

Abstract

The Honey Lake and Fort Sage Mountains faults are active faults in northeastern California. The Fort Sage Mountain normal fault cuts to within 1 km of a previously identified field of precarious rocks that should fall when subjected to moderate strong ground motions. The Honey Lake strike-slip fault strikes within 3-4 km of the same field of rocks. Field mapping, excavations of trenches, and reexamination of natural exposures is used to place limits on the size and frequency of earthquake offsets on the faults. Our observations along the Ft. Sage Mountain fault indicate an earthquake displacement of about 1 m in the Holocene. We suspect that the event is late Holocene but confirmation of that awaits the radiocarbon dating. A ~1 m offset implies an earthquake magnitude of Magnitude 6.8–7.1 using empirical relationships between fault slip and magnitude [Wells and Coppersmith, 1994]. It seems likely that the field of precarious rocks < 1 km away has withstood shaking from such a large earthquake. In addition, we have reconfirmed the multiple mid- to late Holocene earthquake slips on the nearby Honey Lake strike-slip fault. These observations will ultimately provide a quantitative basis to check the accuracy and efficacy of magnitude–source to site distance–magnitude relationships developed on the much shorter period of instrumental recording.

Introduction

The active Honey Lake fault is a northwest-trending, right-lateral fault zone of the northern Walker Lane in California and Nevada (Figure 1). The Honey Lake fault has among the highest slip rates (1.1-2.6 mm/year) and lowest recurrence intervals (~1500 years) of faults in the northern Basin and Range [Wills and Borchardt, 1993]. The nearby Fort Sage Mountains fault is a north-trending normal fault that ruptured during a M 5.6 earthquake in 1950 [Gianella, 1957]. Within a few kilometers of these faults is a zone of precarious rocks (0.2-0.3g toppling acceleration) that are at least several thousand years old [Figure 2 and e.g. *Brune*, 1996; 2002; 2003]. The precarious rocks should be subjected to strong ground motions from earthquakes on the Honey Lake and Fort Sage fault zones. Given that we can estimate the strong motion that would topple the rocks and that we can determine the size and frequency of occurrence of earthquakes on the faults, it is possible to provide important constraints on strong ground motions from normal and strike-slip fault rupture in transtensional environments [e.g. Briggs, et al., 2005; Brune, 1996; 2003]. With that mortivation, graduate students Richard Briggs, Rob Turner, and I have emplaced trenches and examined natural exposures along the two faults to place bounds on the size and timing of earthquakes on the Honey Lake and Fort Sage fault zones. The measurements will provide seismologists the potential to place quantitative bounds on the maximum near-field accelerations that may be produced along normal and strike-slip faults in a transtensional environment. In turn, such knowledge should provide useful constraints on the development of seismic hazard maps [e.g. Briggs, et al., 2005; Brune, 1996; 2002; 2003]. In this report, we first present our observations along the Fort Sage Mountain fault zone and then continue with the same for the Honey Lake fault zone.

Fort Sage Mountains fault zone

We placed two trenches across the Fort Sage Mountains fault zone. An airphoto and surficial geologic map of the two trench sites is shown in Figure 3. The logs of the trenches are shown in Figures 4 and 5. Evidence of a large surface-rupturing earthquake is preserved in both trenches. Surficial relations show that the fault scarp across which we emplaced trenches cuts deposits younger than lacustrine deposits of Lake Lahontan which were deposited about 13,000 radiocarbon years ago [e.g. Adams and Wesnousky, 1998]. The vertical separation of deposits offset during the fault rupture appears at minimum equal to 0.9-1.1 m, which implies an earthquake magnitude of 6.8–7.1 using empirical relationships between fault slip and magnitude [Wells and Coppersmith, 1994]. Thus it appears likely that the nearby precarious rocks, for which ages of "thousands of years" have been inferred [Brune, 2003], survived at least one M 6.8 – 7.1 earthquake on a normal fault that is <1 km away. Confirmation of this awaits absolute dating of the precarious rocks and radiocarbon dates of deposits that are offset by the young fault scarp.

<u>Fort Sage North trench:</u>

The North trench was excavated across a 1.5 -2.1 m scarp preserved in a post-Lake Lahontan (<15,500 years old) fan (**Figure** 3). Here the fault is <1 km from a field of precarious rocks. The trench exposed loose, fine-grained gruess derived from Cretaceous granites upslope. The scarp-forming earthquake can be observed in the trench exposure (Figure 4) as the juxtaposition of fan stratigraphy across a narrow fault zone, and as a single package of scarp-derived colluvium (Unit C1) atop the hanging wall deposits. We have recovered detrital charcoal from the youngest faulted deposits in the hanging wall. The age of the charcoal will provide a maximum age of the scarp-forming earthquake. The detrital charcoal has been submitted for analysis to the AMS C-14 lab at Lawrence Livermore National Laboratory. We have not received the radiocarbon dates in time for the deadline of this final report. The 1950 rupture was not recognized in this trench, possibly due to the small displacement (<20 cm; Gianella, 1957) and relatively poor stratigraphy of the trench exposure.

Fort Sage South trench:

The South trench was excavated across a ~2.0 m scarp preserved on fan deposits that appear older than Lake Lahontan (>15,500 years old) (Figure 3). The trench exposed fluvial sands and gravels and debris flow deposits derived from upslope conglomerates, sandstones, and granites (Figure 5). The exposure contains evidence for two, and possibly three, surface-rupturing earthquakes before 1950. The oldest earthquake is inferred from the mismatch across the fault between the oldest hanging wall deposits (Units 1? and 2?, Figure 5) and the uppermost footwall deposits. The second-oldest pre-1950 paleoearthquake resulted in formation of a ~1.5 m thick colluvial package C1. A period of stability following this event resulted in formation of an argillic soil horizon atop colluvial package C1. The most recent pre-1950 earthquake led to the formation of scarp-derived colluvial package C2. The age of detrital charcoal obtained from scarp-derived colluvial package C2 will ultimately provide a maximum age of the pre-1950 (Figure 5). The 1950 rupture is preserved in the South trench exposure as the extension of fault traces to the surface and possibly as a slightly thickened layer of silt between the main fault strands. In both trenches, the 1950 rupture is difficult to recognize, highlighting the problem of recognizing small-offset earthquakes in exposures with relatively coarse stratigraphy. Also, we discard the hypothesis that the Fort Sage fault repeatedly ruptures in many smaller 1950-style events to produce the colluvial wedges units C1 and C2 because each appears to be a rapidly deposited sequence capped only at their respective surfaces by soil development.

Honey Lake fault zone

Brief overview and background

The Honey Lake fault is a 50 km long strike-slip fault that has accommodated approximately 10 km of offset since its inception [Figures 1 and 6; *Wagner, et al.*, 1989]. The Quaternary history of this fault is for the most part limited to a prior study of a stream cut exposure within Long Valley (Wills and Borchardt, 1993). Interpretation of relationships in the exposure led Wills and Borchardt [1993] to interpret a minimum of four events on the fault postdating deposition of the Mazama ash at 7627 ± 150 cal years B. P. [Zdanowicz, et al., 1999]. Wills and Borchardt [1993] also estimated a slip rate of 1.1 to 2.6 mm per year based on the right-lateral offset of an inset terrace riser where the fault is crossed by Long Valley Creek (**Figure 7**). The Honey Lake fault, like the Ft. Sage Mountains fault, lies near a field of precarious rocks (Figure 2a). We thus extended our study of the Ft. Sage Mountain fault in an attempt to reassess the recurrence rate of surface ruptures and the size of displacements.

Honey Lake Field Site Overview

The Long Valley Creek stream cut that was studied by Wills and Borchardt [1993] is located approximately 4 miles northwest of Doyle, California. (Figure 6). Long Valley Creek generally runs northwards but in this area it takes a meander towards the west, where it cuts across the Honey Lake fault at a very high angle. A terrace riser post-dating Mazama ash is offset here about 19 m [Figure 7 and *Wills and Borchardt*, 1993]. They interpreted the offset to indicate a minimum slip rate across the fault of about 1.1 to 2.6 mm/yr when incorporating the uncertainties associated with the offset measurement. During 1997, the stream cut site was eroded back approximately 7 m during flooding (Cindy Judd, local resident, pers. comm.). We revisited the site in 2004 and cleaned and logged the natural fault exposure. The exposure contains multiple fault strands and numerous deformation features, including fissures, sand dikes and soft sediment deformation. A log of the exposure is shown in Figure 8.

Log and Unit Descriptions of Natural Exposure

The exposure consists of 16 relatively flat-lying units composed primarily of sands and gravels. They are divided based on their specific compositions, sedimentologic or soil characteristics. Units 7, 9, and 11 to 13 extend across the entire exposure, although they are offset across the zone of faulting (Figure 8). The oldest and lowest deposits, Units 15 and 16, are present only northeast of fault strand f. The youngest deposits, units 1, 3 through 6 and 10 are only present southwest of fault strand f.

The composition of Unit 1 is ~65% fine to coarse sand and ~35% fines. It is non-sticky and non-plastic. In the field this unit is massive at the base and grades towards a weak blocky incipient soil at the top. Modern roots are pervasive throughout this unit. The sands are poorly sorted. There is no depositional structure visible. Contact at the base is sharp, occurring over ~2 cm. The top of this unit is the modern ground surface.

Unit 2 is a fine to coarse sand unit with traces of gravel. It contains greater than 95% fine to coarse, predominately medium sands. The grains are angular to rounded, with most subangular. The largest clasts have diameters up to 8mm. The sediments are non-plastic and non-sticky. The base of this unit has slightly coarser sediments but overall there is no well-defined fining upwards sequence. Sorting is moderate to poor. Modern roots are pervasive in this unit. Contact at the base is sharp (<2 cm) and the top of the unit is the ground surface. Based on the geometry of this unit and the slightly coarser base sediments, we infer that it represents a channel cut and fill sequence.

Unit 3 has a distinctive dark brown color and blocky structure. It is composed of ~60% fine to medium, predominately medium sand. It is moderately plastic and moderately sticky. Many fine modern roots are present. It is locally truncated by Unit B. The texture is very uniform.

Unit 4 is a silty sand unit. It is composed of ~55% fine to medium, predominately fine sand and ~45% fines. It is moderately sticky and moderately plastic. It has a massive structure. There are numerous root casts or burrows between 0.5 and 6mm in diameter. Both the top and base of this unit have gradational contacts. Soft sediment deformation is coincident with the fault strand a.

Unit 5 is a very clay rich unit. It is composed of ~90% fines and 10% fine to coarse sand. It is both highly sticky and highly plastic. This unit has a very well developed blocky ped structure. The peds tend to be prolate in shape and range in size from 1x3 cm to 2x6 cm. There are a moderate amount of fine (<1 mm) root casts/burrows. The contact with Unit 4 above is gradational. The basal contact with Unit 6 is sharp to slightly diffuse.

Unit 6 is a thin, silt rich unit. It contains ~55% fine to medium, predominately fine sand and ~45% fines. It is not sticky and is moderately plastic. There are fine (0.5 mm) to large (2 mm) roots present. This unit has a blocky ped structure with ped shapes ranging from orthogonal to prolate. The size of the blocks ranges from 2x3 mm to 5x8 mm. The top 1-2 cm and the bottom 1-2 cm of this unit have distinct red-orange tints. There are sharp contacts at the base (<1 cm) and at the top (<2 cm).

Unit 7 is a fine sand unit. It is composed of ~75% sand and ~25% fines, with traces of gravel. It is slightly sticky and moderately plastic. The grains are angular to subrounded, primarily subangular. There are traces of fine roots present. In places there are two fining upward sequences stacked on each other. This unit is truncated locally by Unit 2. The top contact with unit 3 is gradational, occurring over 5-10 cm. The nature of the basal contact varies. The basal contact is sharp to slightly gradational (>5cm).

Unit 8 is a blocky, silty unit that contains ~60% fine to medium, predominately fine, sand and ~40% fines. It is slightly plastic and non-sticky. This unit is limited in extent. It is only present underneath the incised filled channel represented by Unit 2. The contact at the top is sharp. The contact at the bottom is gradational over ~5 cm.

Unit 9 is a silty sand. It contains ~80% fine to coarse sands and ~20% fines. The grains are subangular to angular. It is non sticky and slightly plastic. The structure is massive in places and blockier in others. In some places there is only weak structure evident or the unit is massive. Where the blocks are more well formed, there are traces of roots and some root casts/burrows. The composition remains fairly uniform across the exposure. The basal contact with Unit 11 is very sharp. The contact with unit 6 above is sharp to slightly gradational.

Unit 10 is only present in the extreme southwest part of the exposure. It is composed of ~90% fine to medium, predominately fine sand and ~10% fines. It is non-plastic and non-sticky. It has a massive structure. Large blocks pluck out when it is scraped. The top and basal contacts are very sharp. Based on its geometry we interpret it to be a channel fill sequence.

Unit 11 is the most distinct unit and the easiest to trace in the exposure. It has components that are coarser in places and finer in others; we interpret that both components were deposited in the same fluvial environment. The coarser component contains ~95% fine to coarse, predominately coarse sand and ~5% gravel. The finer component contains ~80% fine to medium, predominately fine sand and ~20% fines. Both are non-plastic and non-sticky. Towards the southwest part of the exposure this unit is finer, with lenses of coarse sand and gravel. Towards the northeast the unit becomes much coarser. Grains are angular to subrounded, primarily subangular. The larger grains tend to be more rounded. The coarser potions have localized fining upwards sequences. Contacts with units both above and below this unit are sharp.

Unit 12 is a blocky, silty unit. It is composed of ~65% fine sands and ~35% fines. It is moderately plastic and very sticky. This is the blockiest unit present in the exposure. It has numerous root casts and burrows with diameters between 0.5 mm to 2.5 mm. It has a very uniform texture and composition across the exposure. Contacts at the top and at the base are sharp. A carbon sample collected from this layer has been radiometrically dated at 6115 +/- 35 years.

Unit 13 is a fine sand unit. It is composed of ~90-95% fine to medium sand, ~5-10% fines, and a trace of gravel. It is non-plastic and non-sticky. This unit has a massive structure near its base but coarsens upwards. There are lenses of coarser sand with traces of gravel up to 2 cm thick near the top. Where it overlies unit 14 (an ash unit) it contains some large ripped out clasts of ash and reworked ash. There are root casts and burrows between 0.5 and 2 mm in diameter present. Where it is in contact with the water table, this unit tends to hold water and remain damp. The basal contact is sharp except where it overlies the ash unit; there the contact is gradational over 10-15 cm. The top contact is very sharp.

Unit 14 is an ash unit. Wills and Borchardt in 1993 sent it to Sarna –Wojicki, who identified it as the Tsoyawata/Mazama ash (~7,600 ybp). It is only slightly reworked at the base but becomes highly reworked near the top.

Unit 15 is a silty sand. It is composed of ~55% fine to medium sand and ~45% fines. It is slightly sticky and moderately plastic. It is a massive unit that plucks out in small blocks when scraped. It has numerous root casts or burrows up to 6mm in diameter. There are localized areas that appear more sandy, these areas also have fewer root casts / burrows. The contact at the top, with Unit 12, is sharp. The contact at the base, with Unit 16, is gradational over 2-5 cm.

Unit 16 is composed of both 'hard' (more indurated) portions and soft portions. The 'hard' component is composed of 90% fine to medium sand and ~10% fines. The grains are subangular to angular. It is non-plastic and non-sticky. This portion has a higher fine versus medium sand ratio than the soft component. It also contains lenses of coarse sand and gravel. The color is light brown/orange. It interfingers with the soft component, which is composed almost entirely of fine to medium sand with only a trace of fines. It is also non-plastic and non-sticky. The color of the soft component is light gray.

Structural and Stratigraphic Interpretation of Earthquake History

The exposure preserves stratigraphic and structural evidence for a minimum of four fault displacements. The evidence for each is presented below, beginning with the oldest. The fault strands referred to are labeled on Figure 8. Primary evidence for the events is the offset of stratigraphic and soil units. We also observe soft sediment deformation that is probably associated with one of the fault displacements in the exposure.

Event 1

Evidence for the oldest event (Event 1) includes two fault strands that rupture up through Unit 11 and terminate against Unit 9. Fault strand **c** displaces Unit 13 by 20 cm and completely faults Unit 12 out of plane. Fault strand **e** displaces Unit 13 by 15 cm and Unit 12 by 5 cm. There are no scarps located at the upper terminations of these faults. We interpret this to indicate that any scarps that may have formed were eroded away or obscured by continuing deposition of Unit 11 before deposition of Unit 9 began. Charcoal samples were collected from Units 9 and 11. These samples will be dated using AMS C-14 radiocarbon methods and should allow us to bracket the age of Event 1. The sample collected from Unit 11 will provide a maximum age, while the sample collected from Unit 9 will provide a minimum age.

Event 2

Displacement across fault strand **f** is evidence for the 3rd oldest event (Event 2). Strand **f** cuts upwards and displaces all units up through Unit 7. Not all units were displaced equally, and some have as much as 40 cm of apparent vertical offset while others have as little as 5 cm. Event 2 likely exhibited oblique movement since all of the units that it cuts are dropped towards the southwest. In addition, Units 15 and 16 terminate at this strand. We interpret that they were down-dropped below the base of the exposure, faulted out of plane, or a combination of these mechanisms. It is possible to argue that this fault strand represents the youngest event since it propagates to the surface, but other evidence contradicts this. For example, we interpret Unit 6 to represent the remnants of a colluvial wedge that formed as a result of Event 2. If Event 2 were the youngest event, this colluvial wedge should continue southwest and pinch out smoothly. Instead, the wedge is cut by fault strand **d**. This indicates that a younger event must have occurred following Event 2. An in situ charcoal sample was collected from Unit 9. The age of this sample will provide a maximum age for Event 2. Obtaining a constraint on the maximum age of Unit 6 would allow us to determine a minimum age for this event, but so far no charcoal has been found in this unit. We have collected a bulk soil sample and if necessary will submit this to obtain a bulk soil carbon date.

Event 3

The penultimate event, Event 3, is represented by fault strand **a**. This strand cuts upwards through Unit 5 and terminates at the base of Unit 4. The only units showing apparent vertical offsets across fault strand **a** are Units 7 and 9. The other units that it displaces show significant sediment deformation and folding. We interpret the lack of offset along the units to indicate that this fault was primarily strike-slip with very little if any vertical component. Charcoal samples have been collected from Units 4 and 5. These samples have been submitted for AMS C-14 radiocarbon dating and should allow us to bracket the age of Event 3. The sample collected from Unit 5 will provide a maximum age; the sample collected from Unit 4 will provide a minimum age.

Event 4

The youngest event, Event 4, is associated with displacements across fault strands **b** and **d**. Both of these strands cross cut all units up to the weak modern soil (Unit 3). It is possible that they cut this soil also, but due to the very sandy material the soil is forming in it is difficult to determine whether this is the case. The sense of movement for strand **d** is down to the southwest; for strand **b** it is up to the southwest. The units have been down-dropped farther on strand **d** than they have been uplifted on strand **b**; the net effect was the lowering of the elevation of the surface to the southwest. Alternately, these relations could just represent faulting out of plane or a combination of oblique movement and faulting out of plane. We have collected a charcoal sample from Unit 4. If dated, this sample will provide a maximum age for the most recent event. It is likely that we will not be able to accurately date the soil that fault strands **b** and **d** terminate against. This soil would probably date as modern using radiocarbon dating methods. In addition, we could not be sure that any carbon collected from this soil would be truly representative of the age of the deposits since the soil is affected by many modern burrowing insects and animals.

Timing of Displacements

The stratigraphy of the trench in the context of the locations of radiocarbon samples is displayed in an event-horizon diagram in Figure 9. Detrital charcoal samples have been collected from stratigraphic layers bounding each of the earthquake displacements. At this time, we have received analysis of only the oldest in horizon 13, which predates all of the observed earthquake displacements. The detrital charcoal sampled from horizon 13 is dated at 6115 ± 35 radiocarbon years before present. Hence, all four earthquakes occurred subsequent to this time, suggesting an average recurrence interval of about 1500 years. Reception of analyses for the overlying samples will allow limits to be placed on each of the event horizons. The results we observe are in concert with the original findings of *Wills and Borchardt* [1993].

Discussion and Conclusion

The motivation for the research implemented was to place bounds on both the size and frequency of earthquake displacements on two faults located adjacent to a field of previously identified precarious rocks (Figure 2). In this regard, our research has been successful and satisfied the goals of the stated project. Our limitation as of submittal of this report is that we remain waiting for the radiocarbon analysis of submitted detrital charcoal. That withstanding, our observations along the Ft. Sage Mountain fault indicate an earthquake displacement of about 1 m in the Holocene. We suspect that the event is late Holocene but confirmation of that awaits the radiocarbon dating. A ~1m offset implies an earthquake magnitude of Magnitude 6.8–7.1 using empirical relationships between fault slip and magnitude [Wells and Coppersmith, 1994].

It seems likely that the field of precarious rocks <1 km away has withstood shaking from such a large earthquake. This is in contrast to what would be expected from instrumentally derived regressions relating strong ground motion, source to site distance, and earthquake magnitude. In addition, we have reconfirmed the multiple mid to late Holocene occurrence of earthquake slips on the nearby Honey Lake strike-slip fault.

Reports published

This work has resulted in one abstract and was the focus of a Seismological Society of America Annual Meeting field trip in spring 2005. Our results will be written up for submission to a peer-reviewed journal upon receiving the radiocarbon analyses mentioned in the text of this Final Technical Report:

Briggs, R.W., Barron, A.D., Wesnousky, S.G., Brune, J.N, and M.D. Purvance, 2005. Large Earthquakes and Low Footwall Accelerations on the Fort Sage Mountains Normal Fault Zone, Northeastern California. Talk presented at the 2005 Seismological Society of America Annual Meeting.

References

Adams, K. D., and S. G. Wesnousky (1998), Shoreline processes and the age of the Lake Lahontan highstand in the Jessup Embayment, Nevada, *Geological Society of America Bulletin*, *110*, 1318-1332.

Briggs, R. W., et al. (2005), Large earthquakes and low footwall accelerations on the Fort Sage mountains normal fault zone, northeastern California, *Abstracts of Annual Meeting of the Seismological Society of America*.

Brune, J. N. (1996), Precariously balanced rocks and ground-motion maps for southern California, *Bulletin of the Seismological Society of America*, *86*, 43-54.

Brune, J. N. (2002), Precarious-rock constraints on ground motion from historic and recent earthquakes in southern California, *Bulletin of the Seismological Society of America*, *92*, 2602-2611.

Brune, J. N. (2003), Precarious rock evidence for low near-source accelerations for trans-tensional strike-slip earthquakes, *Physics of the Earth and Planetary Interiors*, *137*, 229-239.

Gianella, V. P. (1957), Earthquake and faulting, Fort Sage Mountains, California, December 1950, *Bulletin of the Seismological Society of America*, *47*, 173-177.

Wagner, D. L., et al. (1989), The Honey Lake fault zone, northeastern California, its nature, age and displacement, *EOS Transactions*, *70*, 1358.

Wells, D. L., and K. J. Coppersmith (1994), New Empirical Relationships among Magnitude, Rupture Length, Rupture Width, Rupture Area, and Surface Displacement, *Bulletin of the Seismological Society of America*, *84*, 974-1002.

Wills, C. J., and G. Borchardt (1993), Holocene Slip Rate and Earthquake Recurrence on the Honey Lake Fault Zone, Northeastern California, *Geology*, *21*, 853-856.

Zdanowicz, M. A., et al. (1999), Mount Mazama eruption: Calendrical age verified and atmospheric impact assessed, *Geology*, *27*, 617-620.

Ll bar

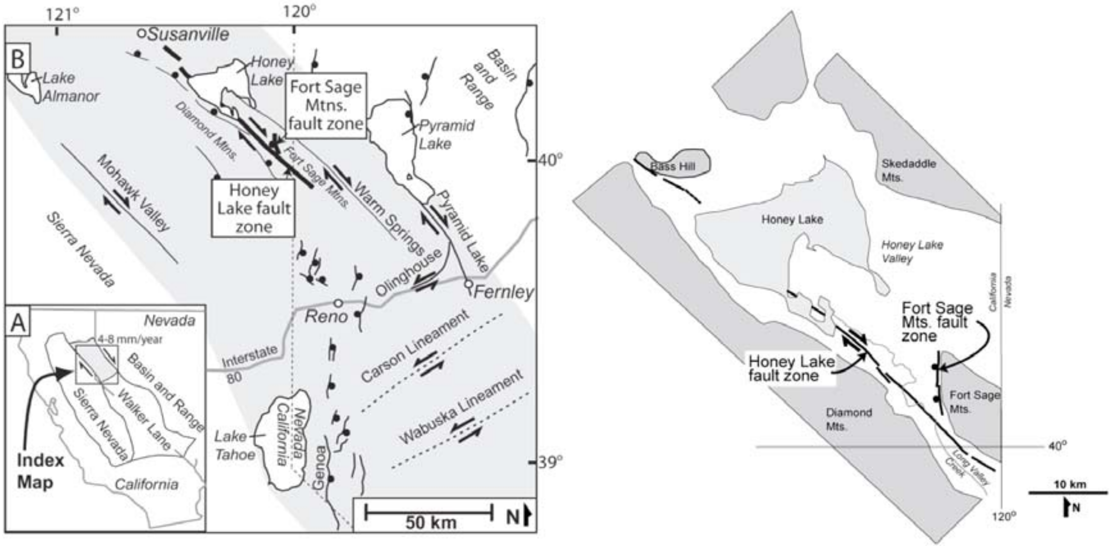

Figure 1. Location maps of the Honey Lake and Fort Sage Mountains fault zones. Shaded area on left figure is location of the northern Walker Lane. Geodetic studies show about 1 cm/yr of NW-directed, right-lateral shear accumulates across the northern Walker Lane near the latitude of Reno.

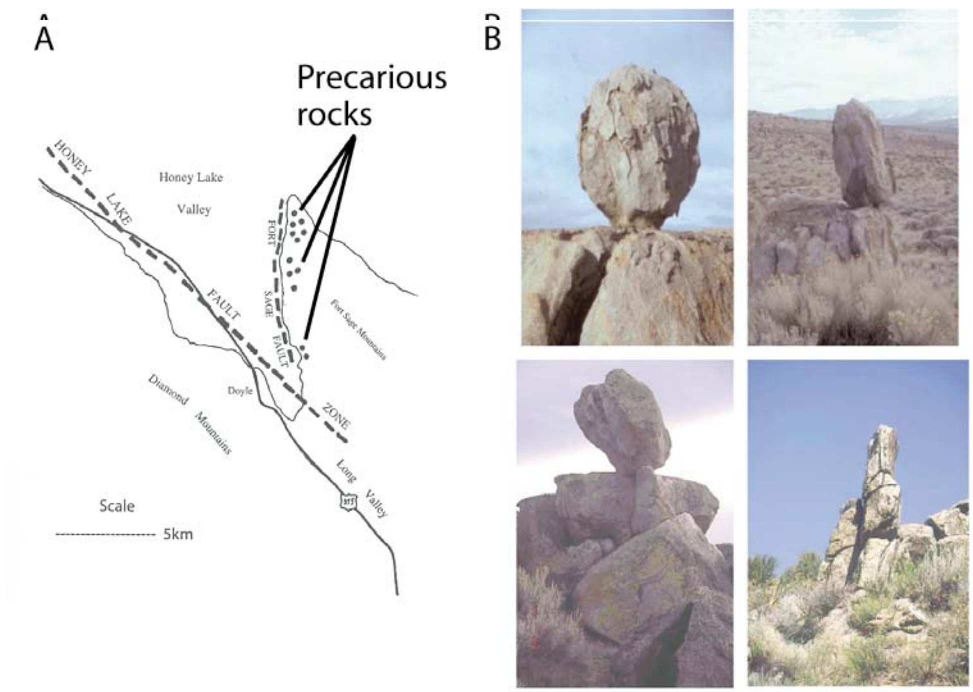

Figure 2. (A) Map showing location of precarious boulders with respect to Honey Lake and Fort Sage Mountains fault zones. (B) Photographs of typical precarious rocks in the Fort Sage Mountains. Toppling accelerations are 0.2-0.3 g. Figure adapted directly from Brune [2003].

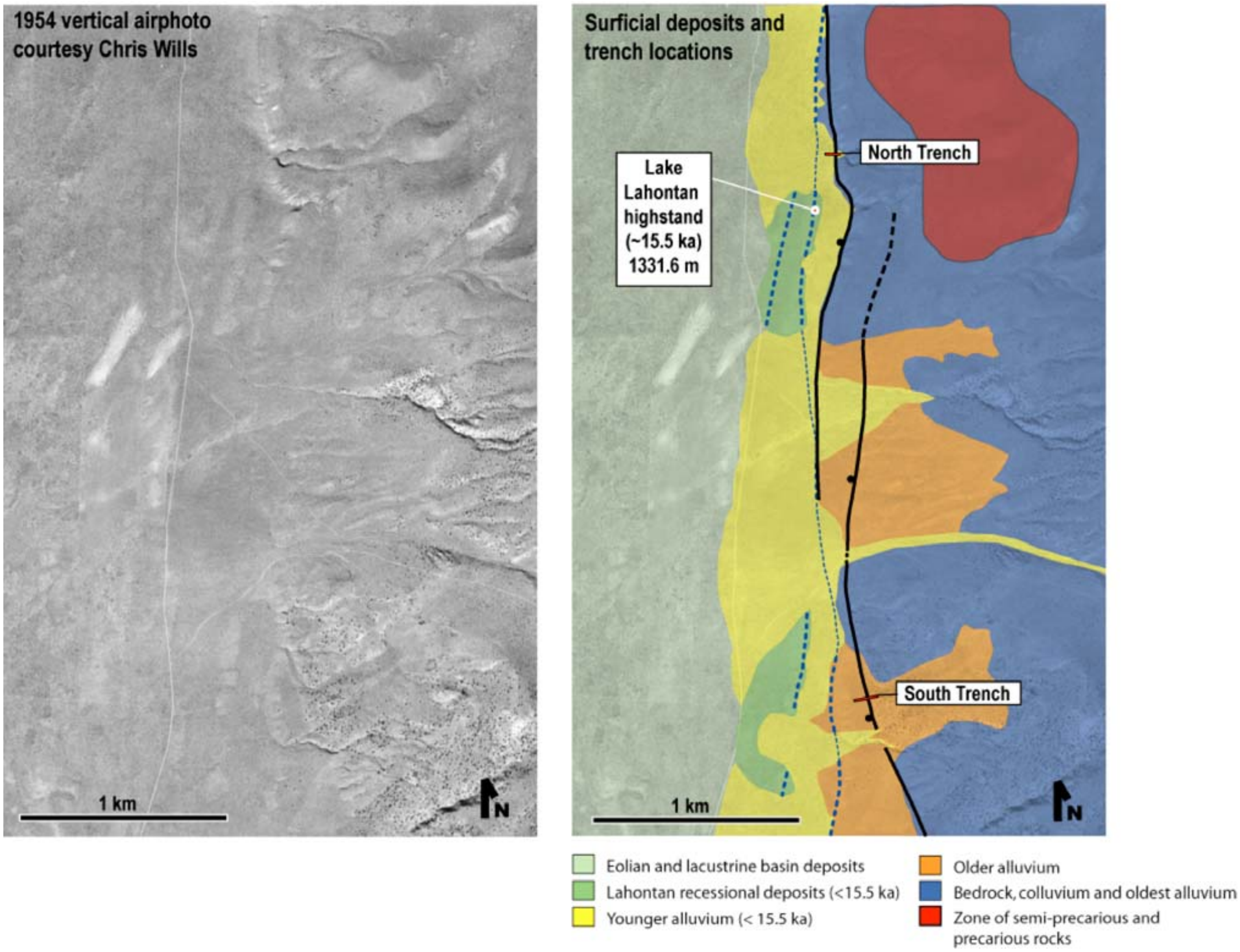

Figure 3. Trench locations and surficial deposits along the Fort Sage Mountains fault zone.

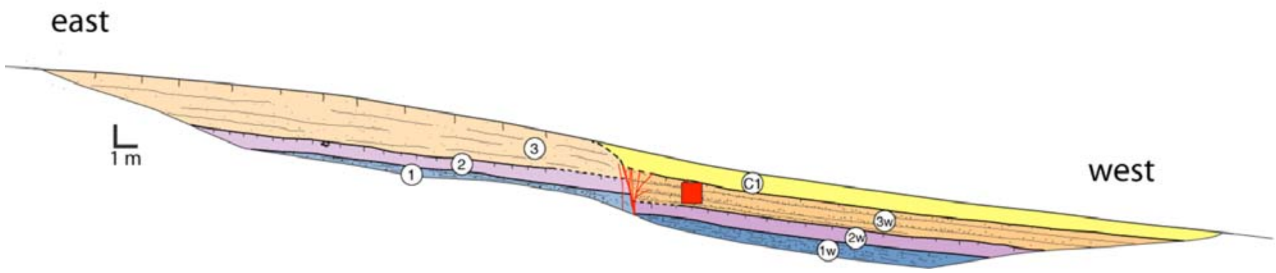

Figure 4. Simplified trench log of Fort Sage North trench. Fault zone shown in red. Units are **1-**poorly sorted silt to small cobble in intercalated debris flow and fluvial deposits; **2-**moderately sorted sand to small pebbles of fluvial origin with weak soil development at top of deposit; and **3-**moderately sorted, weakly stratified silt to small pebbles, highly bioturbated. Hanging wall units (**1W – 3W**) are significant facies changes of footwall units and are in general much better sorted with more prominent bedding. The mismatch between hanging wall and footwall deposits implies a component of oblique slip. The red square denotes the location of radiocarbon sample RWB-FSN-C1 which will provide a maximum age of the fault displacement that led to formation of colluvial package **C1**.

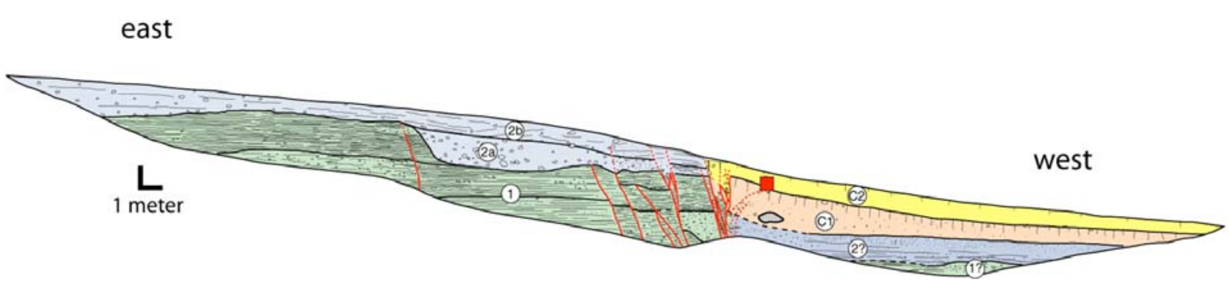

Figure 5: Simplified trench log of Fort Sage South trench. Fault strands shown in red. Units are **1**-fluvial sand and gravel in thin, continuous subhorizontal laminae with occasional crossbedding; **2a**-poorly sorted channelized debris flow deposit; **2b**-moderately sorted fluvial sands and gravels, high component of gruess, exhibiting much less well-defined bedding than unit 1; **1?**-possible match for unit 1 in hanging wall but in general much more poorly sorted and without distinctive well-defined bedding; **2?**-possible match for 2b but with much smaller gruess component; **C1**-colluvial package; **C2**-colluvial package. The red square denotes the location of radiocarbon sample RWB-FSN-C1 which will limit the age fault displacement that led to formation of colluvial package C2. Facies mismatches across faults cutting Unit 1 suggest a substantial oblique component of slip

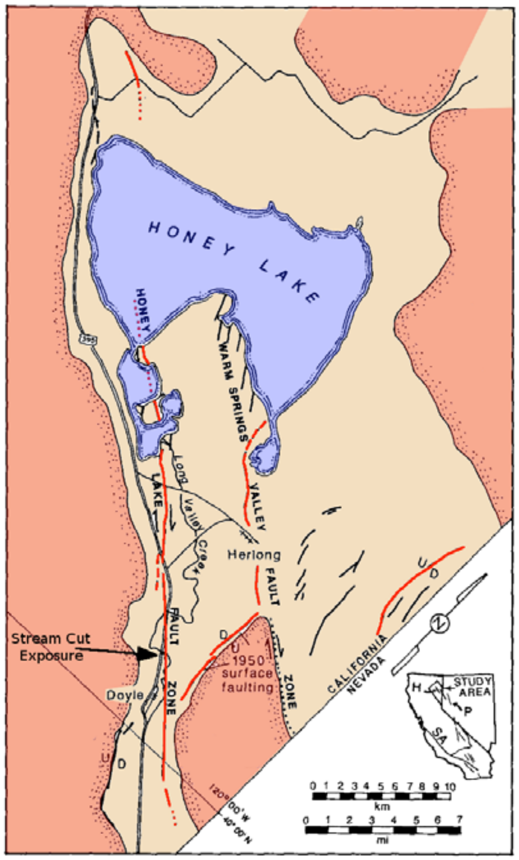

Figure 6. Regional context and location of stream cut exposure along Honey Lake Fault Zone [adapted from Wills and Borchardt, 1993].

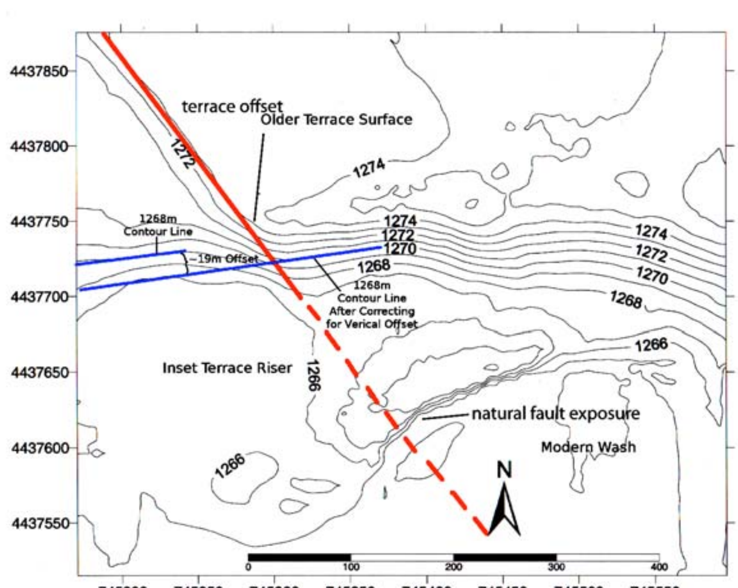

Figure 7. Contour map of Honey Lake study site showing context of offset terrace riser and natural fault exposure. A best estimate of the offset terrace riser is 19 m.

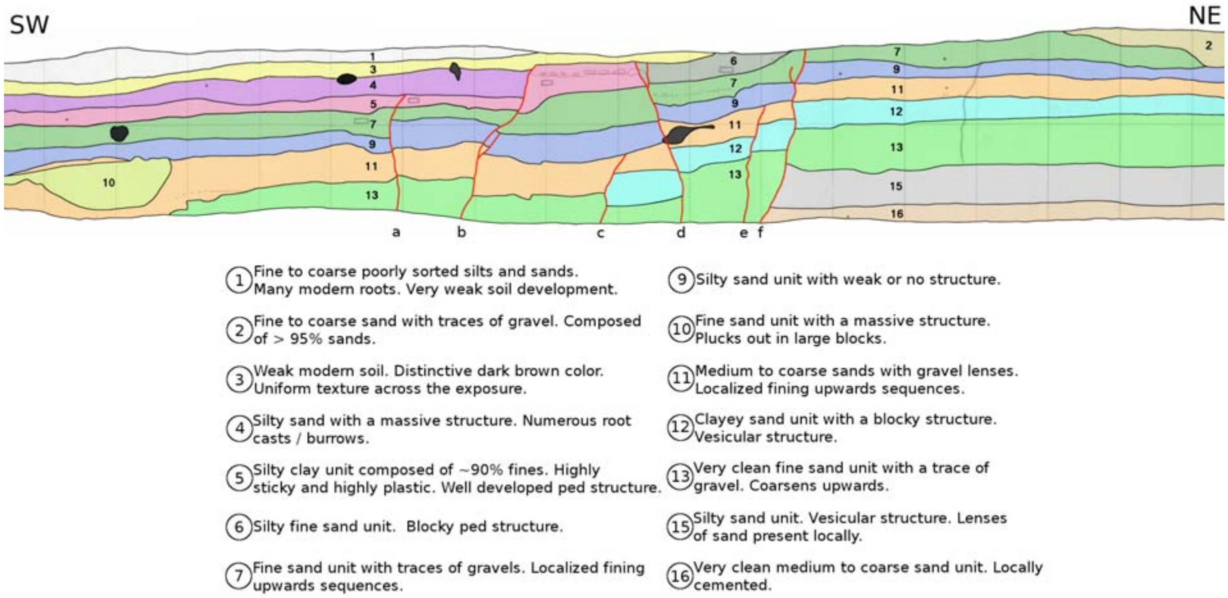

Figure 8. Log and brief unit descriptions of the natural exposure of the fault zone on Long Valley Creek.

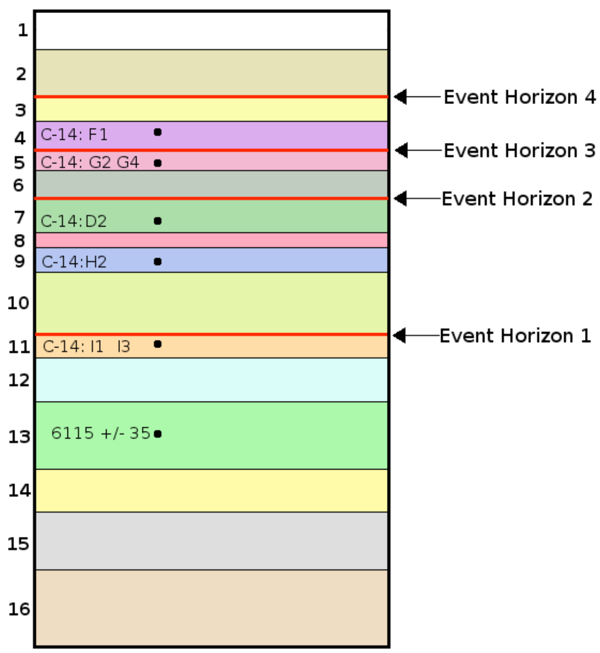

Figure 9. Event horizon diagram shows location of radiocarbon samples collected. At this time, we have received results only for one sample in unit 13. The others are currently being processed.

-